# Crystallinity and Crystalline Confinement of the Amorphous Phase in Polylactides

*Jose-Ramon Sarasua,* Ester Zuza, Nagore Imaz, Emilio Meaurio*

**Summary:** Stereorregular polylactides such as poly (L-lactide) (PLLA) or poly (D-lactide) result from polymerization of optically pure lactides and are semicrystalline. Optically non-active poly(D,L-lactide) (PDLLA) can be regarded as random or atactic copolymers, show a random moiety distribution, and are completely amorphous. In this work three phases, comprising mobile amorphous fraction (MAF, $\chi_{MA}$), rigid amorphous fraction (RAF, $\chi_{RA}$) and crystalline fraction ($\chi_c$) were determined in PLLA. It will be shown that RAP fraction not only elevates Tg but also increases the dynamic fragility (m) of polylactide chains around the Tg. These results agree with reported cases in which topologycal constraints inhibit longer range dynamics and suggest a smaller length scale of cooperativity of chains in confined environments.

**Keywords:** biodegradable; crystallinity; polyester

## Introduction

In many aspects there is still a lack of understanding of the fundamentals of physical chemistry that govern the segmental relaxation of polymer chains in both non-confined and confined environments. Nonetheless, it is well established that constraints of polymer chains caused by crystallinity lead to an increase in the temperature of the glass transition, for chains find a growing hindrance to relax. Since macromolecules are longer than the crystal lamellae are thick, they can cross the phase boundaries and cause various degrees of coupling; on weak coupling, the dynamics of the non-crystalline segments shows usually a broadening of the glass transition range, yet on stronger coupling the non-crystalline material may also show a distinct glass transition, at higher temperature of the bulk amorphous phase due to a rigid amorphous phase.[1]

The occurrence of the glass transition in polymers is associated to cooperative motion of macromolecular chain segments. Cooperative segment length ($\xi$) results to be in the range 1–3 nm at the glass transition temperature depending on the glass forming polymer.[2] Although there is still no unambiguous answer as to whether the chain mobility is increased or decreased by constraints, the observation that the Tg of polymeric systems in confined environments may be suppressed[3,4] supports the idea that cooperativity of chain motion is impeded when the dimension of the topological constraint (d) is smaller than $\xi$.

The glassy state is unstable because a glass is continually relaxing towards equilibrium and therefore the different related properties are also changing. The dynamic fragility, concept introduced by Angell,[5] accounts for the easy with which this transition is completed. A polymer is defined dynamically fragile when there is little impediment for segmental relaxation of chains and carries rapidly a drastic change in properties (viscosity, modulus, etc.) at the Tg, characteristic of each polymer. During the last years the fragility dilemma of liquids has raised research interests and particular efforts have been carried out to systematize the different polymers according to the fragility parameter.[6,7]

University of the Basque Country (EHU-UPV), Faculty of Engineering, Alameda de Urquijo s/n, 48013 Bilbao, Spain
E-mail: jr.sarasua@ehu.es

The dynamic fragility is related to the deviations from simple Arrhenius temperature dependence of the relaxation process. According to the Vogel-Fulcher-Tammann-Hesse (VFTH) equation the relaxation time, $\tau$, is given in the following way:[8]

$$\tau = \tau_0 * e^{\left(\frac{B}{T-T_0}\right)}, \quad (1)$$

where $\tau_0$, $B$, and $T_0$ are positive constants. From the VFTH equation a convenient measure for the dynamic fragility (m) is related to the steepness index in the glass transition as follows:

$$m = \left.\frac{d\log\tau}{d(T_g/T)}\right|_{T=T_g} = \frac{BT}{(T_g - T_0)^2}, \quad (2)$$

The Williams-Landel-Ferry equation is mathematically equivalent to the VFTH equation; it is constructed in order to eliminate the pre-exponential factor of VFTH equation and reflects the temperature dependence in the following manner:[9]

$$\log\frac{\tau}{\tau_0} = \log a_T = \frac{-C_1(T - T_g)}{C_2 + T - T_g}, \quad (3)$$

$C_1$ and $C_2$ are material constants and the fragility parameter can be calculated as follows:[9]

$$m = \left.\frac{d(\log a_T)}{d(T_g/T)}\right|_{T=T_g} = \frac{T_g C_1}{C_2}. \quad (4)$$

Dynamic fragility of polymers has been reported to fall inside a m = 40–200 range.[10] If m has a high value, then the material is classified as a fragile liquid, whereas when m is low it is a strong glass former. In this work we have conducted a molecular dynamics' analysis by DMA in order to study the segmental relaxation of polylactide chains around the Tg in a fully amorphous medium and in presence of a crystalline-confined environment.

The comparison of the dynamic fragility parameter in an unconfined bulk amorphous phase and in a partly crystalline confined one will allow us to draw straightforward conclusions on the different segmental cooperativity of polylactide chains during the relaxation processes involved in both cases. In a previous work on the conformational behavior in PLLA films,[11] we concluded that the interphase seemed to extend over the whole interlamellar region showing the features of a semiordered metastable phase. Considering a single mobile amorphous phase in PDLLA and the presence of mobile and rigid amorphous fractions in PLLA, it seems reasonable to foresee a different molecular segmental dynamics around the Tg in both cases.

## Experimental Part

PDLLA and PLLA were supplied by Purac Biochem (The Netherlands). The molecular weight of both polymers was measured viscometrically in a Ubbelohde type viscometer in chloroform at 30 °C. Values of $M_v = 3.8 \cdot 10^5$ g/mol and $M_v = 3.2 \cdot 10^5$ were obtained using the appropriate Mark-Houwink constants for each polymer.[12]

In the present work both amorphous PDLLA and semicrystalline PLLA were used as starting materials to obtain 1mm thick sheets by compression molding. All samples were melted at 200 °C and rapidly quenched in water. PLLA samples were further crystallized whether by annealing at 80 °C for 3h after quenching or by slow cooling from the melt into the plates of the press.

Thermal analysis was carried out on a DSC from TA Instruments, model DSC 2920. Approximately 5–10 mg of each blend was weighed and sealed in an aluminium pan. DSC scans were performed on sheet samples with a scan rate of 20 °C/min. Glass transition temperatures were measured as middle point values.

Rectangular specimens were cut from compression molded sheets and tested in a dynamic mechanical analyzer DMA/SDT A861 from Mettler-Toledo (shear mode). To obtain the master curves and dynamic fragility of materials the measurements were conducted in the DMA between 20 and 0.01 Hz in isothermal conditions from Tg-30 °C to Tg + 30 °C every 3 °C. Master

 

curves for the storage modulus G′ and tan $\delta$ were composed by shifting the values obtained in isothermal conditions along the frequency scale according to the time-temperature principle.[9]

## Results and Discussion

Figure 1 shows the DSC thermogram of PDLLA and PLLA samples conformed from the melt without or with thermal treatment. PDLLA shows the heat jump corresponding to the Tg at 54 °C. The glass transition of PLLA-WQ appears at 61 °C followed by a typical cold crystallization peak at 92 °C and a melt fusion peak at 181 °C, which is accompanied by a small exothermal event just before the melting at 161 °C. This second exothermal peak has been already reported elsewhere and has been attributed to a recrystallization into $\alpha$ polylactide crystal polymorph of higher perfection.[13] Looking at the two curves of the bottom corresponding to annealed and slowly cooled PLLA samples, in addition to the suppression of cold crystallization behavior due to the higher crystallinity of the samples, it is remarkable a Tg increase of 10–14 °C with respect to the non-treated quenched PLLA-WQ and an increase of 17–21 °C with respect to fully amorphous PDLLA.

Crystallinity degree ($\chi_c$) of PLLA was determined using a value of 106 g/mol for melting enthalpy of 100% crystalline polylactide according to Equation 5.[14] As can be observed the heat capacity change at Tg reduces significantly with crystallinity and RAF. Equation 6 and Equation 7 can be proposed to account for rigid amorphous and mobile amorphous fractions respectively:[15]

$$\chi_c = \frac{\Delta H_m - (\Delta H_c - \Delta H_{rc})}{\Delta H_m^0} \quad (5)$$

$$\chi_{RA} = 1 - \chi_c - \frac{\Delta C_p}{\Delta C_p^0} \quad (6)$$

$$\chi_{MA} = 1 - \chi_c - \chi_{RA} \quad (7)$$

Table 1 reports the thermal properties obtained for PDLLA and PLLA. It is observed that mobile amorphous phase is only present in PDLLA and rigid amorphous fraction increases with crystallinity in PLLA. Even quenched in water, PLLA shows a non-negligeable amount of crystalline and rigid amorphous fractions. Finally PLLA annealed samples show both higher crystallinity and RAF than samples crystallized from the melt.

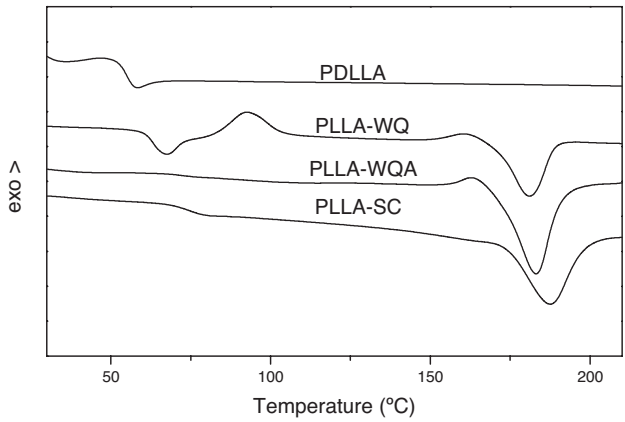


***Figure 1.***
DSC curves of PDLLA and PLLA with different thermal treatments. PDLLA: quenched in water from the melt, not annealed; PLLA-WQ: quenched in water from the melt, not annealed; PLLA-WQA: quenched in water from the melt and annealed at 80 °C for 3h; PLLA-SC: slowly cooled from the melt inside the mold.

 

***Table 1.***
Thermal properties of polylactides.

| | $T_g$ (°C) | $\Delta C_p$ ($Jg^{-1}°C$) | $\Delta C_p/\Delta C_p^0$ | $\chi_c$ | $\chi_{RA}$ | $\chi_{MA}$ |
|---|---|---|---|---|---|---|
| PDLLA | 54 | 0.62 | 1 | 0 | 0 | 0 |
| PLLA-WQ | 61 | 0.45 | 0.274 | 0.107 | 0.167 | 0.726 |
| PLLA-SC | 74 | 0.30 | 0.516 | 0.265 | 0.251 | 0.484 |
| PLLA-WQA | 71 | 0.10 | 0.839 | 0.388 | 0.451 | 0.161 |

$\Delta C_p$: specific heat change at Tg; $\Delta C_p^0$: specific heat change at Tg in fully amorphous polylactide; $\Delta H_{c1}$: exothermal enthalpy change (cold crystallization peak); $\Delta H_{c1}$: exothermal enthalpy change (just before melting), $\Delta H_m$: melting enthalpy.

Figure 2 represents the master curve for PLLA. Master curves were built and the shift values ($a_t$) obtained for PLLA and PDLLA using the DMA experiments conducted at different temperatures and frequencies according to the WLF theory (Equation 3). $C_1$ and $C_2$ constants were deduced by WLF equation using the shift values ($a_t$) experimentally obtained. Finally the dynamic fragility parameter (m) was calculated with Equation 4. Table 2 reports the fragility values taking into account the fitting errors.

Angell's plot in which log $a_t$ is represented in ordinates versus Tg/T in abscissa is also a good method to compare the segmental dynamics of different glass forming liquids. The Angell's plots for PDLLA and PLLA are presented in Figure 3. Angell's plot in which log $a_T$ is represented in ordinates versus $T_g/T$ in abscissa is also a good method to compare

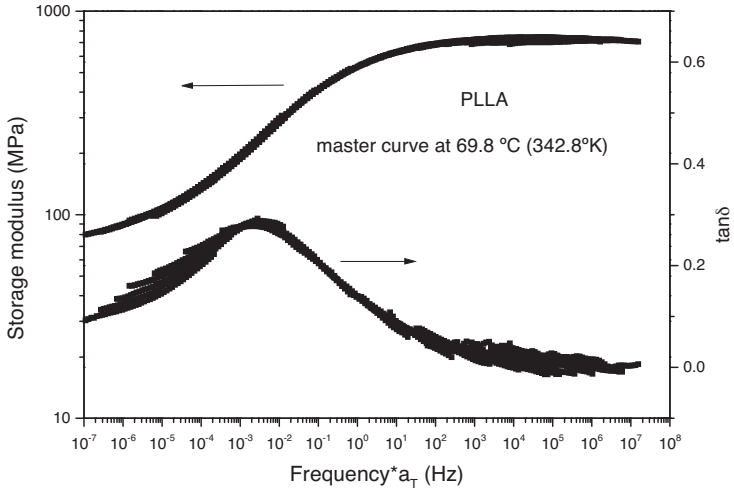


***Figure 2.***
PLLA-WQA: master curve at 69.8 °C.

***Table 2.***
Dynamic fragility (m) of polylactides, taken into account the fitting errors.

| PLLA | PLLA_min | PLLA_max | PDLLA | PDLLA_min | PDLLA_max |
|---|---|---|---|---|---|
| $C_1 = 12.73787 \pm 0.72637$ | $C_1(-)^*T_g/C_2(+)$ | $C_1(+)^*T_g/C_2(-)$ | $C_1 = 10.32397 \pm 0.53822$ | $C_1(-)^*T_g/C_2(+)$ | $C_1(+)^*T_g/C_2(-)$ |
| $C_2 = 29.12788 \pm 2.44863$ | $m = 130.4$ | $m = 173.0$ | $C_2 = 48.61025 \pm 3.86054$ | $m = 61.1$ | $m = 79.5$ |

 

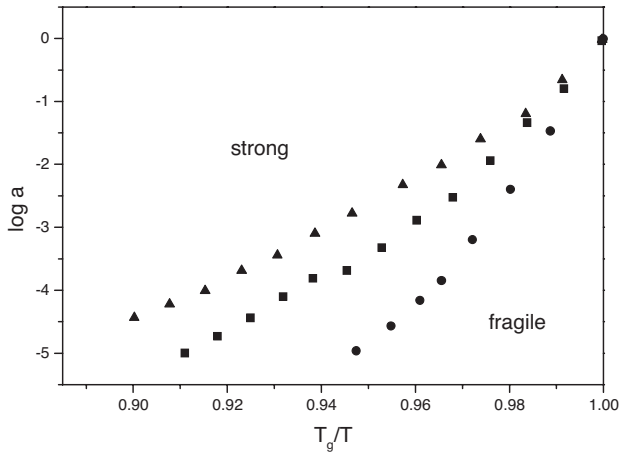


***Figure 3.***
Angell's plot: PDLLA (▲), PLLA-SC (■) and PLLA-WQA (●).

the segmental dynamics of different glass forming liquids. Materials showing near Arrhenius behavior are strong glass formers and hence the deviation from linearity is an indication of dynamic fragility. Taking the derivative of the curves at $T_g/T = 1$ the following dynamic fragility values were obtained respectively for PLLA-WQA and PDLLA: $m = 128.4$ and $m = 75.5$.

## Conclusion

In summary, our results show that fully amorphous PDLLA is a stronger glass former than semicrystalline PLLA. Three phases, comprising mobile amorphous fraction (MAF), rigid amorphous fraction (RAF) and crystalline fraction ($\chi_c$) were found in poly (L-lactide) (PLLA). The amount of RAP was established after isothermal cold crystallization or by non-isothermal cooling of samples from the melt. Dynamic mechanical analysis (DMA) of PLLA after aging at 50 °C revealed a partial relaxation of the rigid amorphous phase giving rise to double Tg behaviour. The lower temperature tan $\delta$ peak in PLLA is coincident with the Tg of PDLLA and hence confirms is a result of segmental mobility of non-confined polylactide chains.

RAP fraction not only elevates Tg but also increases the dynamic fragility of polylactide chains around the Tg. These results are novel and agree with recently reported correlations between dynamic fragility and glass transition temperature for different classes of hydrogen bonding organics and polymeric glass formers showing an increase in m with increasing Tg.[10] Although impediments for segmental mobility are associated to a Tg increase in polymeric systems, segmental dynamics around the Tg, i. e. the steepness or easiness with which a glass former relaxes (fragile liquid behavior) increases with crystalline confinement. It is proposed that crystallinity is acting in polymeric systems as a topologycal constraint, in a similar way as silicate layer surfaces of exfoliated nanocomposites,[3] inhibiting longer range dynamics and hence allowing smaller length scale of cooperativity.

*Acknowledgements:* The authors are thankful for financial support from Basque Government — Dept. of Industry, Trade and Tourism (Project IE03-105), University of the Basque Country (Project UPV 05/130) and MEC (Project MAT 2006-13436-C02-01).

[1] B. Wunderlich, *Prog. Polym. Sci.* **2003**, *28*, 383–450.
[2] D. Cangialosi, A. Alegría, J. Colmenero, *Europhys. Lett.* **2005**, *70*, 614–620.

 

[3] E. Manias, V. Kuppa, D.-K. Yang, D. B. Zax, *Colloids and Surfaces, A: Physicochemical and Engineering Aspects* **2001**, *187*, 509–521.
[4] J. Pak, M. Pyda, B. Wunderlich, *Macromolecules* **2003**, *36*, 495–499.
[5] C. A. Angell, *Journal of Non-Crystalline Solids* **1991**, *131*, 13–31; *Science* **1995**, *67*, 1924.
[6] D. Huang, G. B. McKenna, *Journal of Chemical Physics* **2001**, *114*, 5621–5630.
[7] R. Bohmer, K. L. Ngai, C. A. Angell, J. Plazek, *Journal of Chemical Physics* **1993**, *99*, 4201–4209.
[8] H. Vogel, *J. Physik. Z.* **1921**, *22*, 645; G. S. Fulcher, *J. Am. Ceram. Soc.* **1925**, *8*, 339; G. Tammann, W. Z. Hesse, *Anorg. Allgem. Chem.* **1926**, *156*, 245.
[9] M. L. Williams, R. F. Landel, J. D. Ferry, *Journal of the American Chemical Society* **1955**, *77*, 3701–3707.
[10] Q. Qin, B. McKenna, *Journal of Non Crystalline Solids* **2006**, *352*, 2977–2985.
[11] E. Meaurio, N. López-Rodríguez, J. R. Sarasua, *Macromolecules* **2006**, *39*, 9291–9301.
[12] A. Schindler, D. H. Harper, *J. Polym. Sci. Polym. Chem. Ed.* **1979**, *17*, 2593.
[13] Y. Ohtani, K. Okumura, A. Kawaguchi, *Journal of Macromolecular Science, Physics* **2003**, *B42*, 875–888.
[14] J. R. Sarasua, R. E. Prud'homme, M. Wisniewski, A. Le Borgne, N. Spassky, *Macromolecules* **1998**, *31*, 3895.
[15] M. Arnoult, E. Dargent, J. F. Mano, *Polymer* **2007**, *48*, 1012–1019.

 